



Article

Performance of the Steel Fibre Reinforced Rigid Concrete Pavement in Fatigue

Chee Keong Lau ^{1,*}, Amin Chegenizadeh ¹, Trevor N. S. Htut ² and Hamid Nikraz ¹

¹ School of Civil and Mechanical Engineering, Curtin University, Kent Street, Bentley, WA 6102, Australia; amin.chezenizadeh@curtin.edu.au (A.C.); h.nikraz@curtin.edu.au (H.N.)

² ETTOL Engineered Solutions, 1/41 Catalano Circuit, Canning Vale, WA 6155, Australia; trevor.htut@ettol.com.au

* Correspondence: cheekeong.lau@curtin.edu.au

Received: 11 September 2020; Accepted: 14 October 2020; Published: 16 October 2020



Abstract: Four-point bending fatigue experimental work was conducted on specimens that were cut from slabs to examine the fatigue life of concrete pavements. The variables considered were the volume fraction of fibres added in plain or steel bar reinforced concrete. It was found that the strain-based approach to fatigue testing on scaled-down concrete pavements is suitable to investigate the fatigue performance of scaled-down thin rigid pavements. The addition of fibres at 0.5% volume fraction in concrete improved the fatigue life by at least 135% and reduced the energy dissipated per cycle by 74%. As the volume fraction of fibres increased, it was found that the fatigue life of rigid pavements improved; total energy dissipation also increased but the energy dissipated per cycle was reduced in concrete pavements. This is due to the crack bridging effect of fibres that reduces the microcracking of concrete. The energy dissipation per cycle from fracture energy does not remain constant for rigid pavements under fatigue testing as it was found that the type of reinforcements influences the quantity of energy dissipated. Finally, hybrid reinforced pavements with both steel bars and fibres yielded the best performance in fatigue, with the highest number of fatigue cycles and lowest energy dissipated per cycle.

Keywords: apparent volume of permeable voids; energy dissipation; fatigue; four-point bending; rigid pavements; ordinary Portland cement; steel fibres

1. Introduction

Concrete has been widely applied as the construction material for structural elements in infrastructures that include road pavements, ground slabs, supporting columns, bridge girders and other structural elements. In general, many of these structures are under significantly lower loads that are below the ultimate load of the structure; however, these loads are being exerted on a cyclic basis [1]. Similar to soils, cyclic loading has a significant effect as it can lead to fatigue failure, where fatigue damage is one of the most common modes of failure in concrete structures [2,3]. It is believed that fatigue damage accounts for up to 80% of structural failures [4]. As the cyclic loading is exerted on a concrete structure, microcracks are initiated and propagated through the concrete matrix, with these cracks accumulating over a long period or large numbers of cycles. Eventually, macrocracks will start to form, with a sufficient amount of microcracks accumulating over time, and this will lead to large and unsightly cracks appearing on the structure or structural failure [5,6].

The prevention of fatigue cracks has been considered as one of the major design criteria of pavements [7]. Generally, pavements consist of three main layers, which are (i) surface course, (ii) base course and (iii) subgrade/existing soil. The surface course can be constructed as either flexible pavement with asphalt or rigid pavement with concrete slabs. The function of rigid pavements differs from flexible pavements as rigid pavements are designed to spread the load over a larger

area [7]. The concrete slabs in rigid pavements are designed to provide sufficient rigidity and, more importantly, flexural strength to support the moving loads and the insufficient capacity of the subgrade. Flexible pavements are known to have self-healing capabilities [8] but rigid concrete pavements are lacking in a similar type of dissipated heat-based self-healing capacity that flexible pavements have. Hence, the crack control of the concrete slabs has increased importance, where concrete rigid pavements are reinforced with steel. The use of fibres would help to control the crack propagation and improve fatigue performance. Thus, the presence of fibres in the brittle concrete slab can improve its poor tensile performance and increase flexural strength. This is because fibres can improve concrete performance or serviceability via the crack bridging mechanism by fibres. The post cracking tensile capacity of the fibre reinforced concrete occurs via the matrix–fibres mechanical friction and the fibre anchorage. Due to the crack bridging behaviour of fibres, the addition of fibres has been an attractive option in the industry to improve the performance of concrete structures [9,10]. It is known that the use of fibres in pavements has led to numerous improvements, such as the reduction in shrinkage, temperature-induced stresses and crack formation [11]. With numerous benefits of fibre reinforced concrete, the application of joint-free pavements is possible via the combined use of fibres and conventional steel reinforcements in concrete pavements. Joint-free pavements offer additional benefits such as the reduction of construction time and cost substantially by decreasing the need for the construction of dowels in pavements [12]. Therefore, this highlights the importance of concrete fatigue testing with both fibres and conventional reinforcements.

The effect of fibres in the concrete matrix in fatigue has been studied extensively [13–16]. While the stress-based approach in fatigue is commonly used in brittle material such as concrete [1,17], it is known that the stress-based loading condition causes heightened levels of crack propagation in comparison to strain-controlled [18]. As this study is focused on the fatigue behaviour of warehouse pavements that are comparably thinner than beams, strain-controlled would be more suitable [1]. The fatigue testing regime's loading mode of fatigue testing has a significant influence on the degradation process. The fatigue testing of concrete via crack mouth opening displacement (CMOD) beams or structural level fatigue testing is generally more difficult to conduct [12,15,19].

With the consideration of concrete material property, this study presents a novel approach in the fatigue investigation with the application of strain control at the cracking strain of concrete for a scaled-down concrete common residential or warehouse pavement. In accordance with AS3727.1-2016 [20], the typical thickness of residential or warehouse pavements is between 75 and 150 mm, which is significantly thinner than most structural beams and slabs in infrastructures or commercial buildings. Thin slabs may have a significant impact on the orientation of the fibres as fibres have a higher likelihood to align with certain orientations in thin slabs than larger structural elements. The methodology proposed in this study adopts a similar methodology in testing as asphalts, with the same equipment able to be used for evaluating the performance of thin concrete pavements. The use of the asphalt testing provides a more applicable and consistent testing regime as the same equipment may be used for the assessment of thin concrete rigid pavements in fatigue. For this study, the cracking strain of the rigid pavements in residential or warehouse applications was selected for fatigue testing to investigate the influence of fibres in fatigue. The cracking strain of the concrete is defined as the strain level exerted to cause concrete to crack at the tension side of the concrete. This is because fibres in concrete do not provide any tensile capacity until the concrete is cracked [21]. The fibres are only engaged after the concrete is cracked. To investigate the effectiveness of the cracking strain-based testing on thin rigid concrete pavements, this study tested and evaluated the fatigue performance in unreinforced concrete and reinforced concrete with either fibre, longitudinally reinforced steel reinforcements or both.

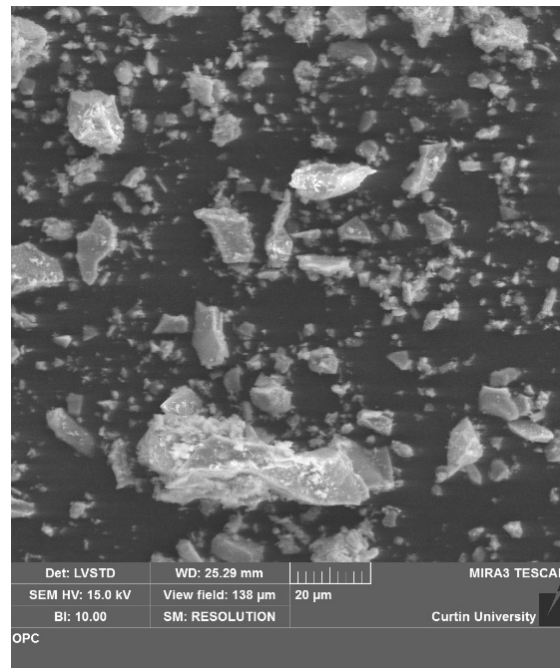
2. Specimen Preparation

The aggregates of the concrete consisted of river sand crushed basalt gravel with a maximum diameter of 1.18 and 7 mm. The Portland cement was obtained from a local supplier, with a specific gravity of 2.9 and a bulk density of 1300 kg/m³. The bulk oxide composition is listed in Table 1.

Table 1. Bulk oxide composition (wt %) and loss of ignition at 1000 °C of the Portland cement.

| Elemental Oxide | Al ₂ O ₃ | CaO | Fe ₂ O ₃ | MgO | Na ₂ O | SO ₃ | SiO ₂ | LOI |
|-----------------|--------------------------------|------|--------------------------------|-----|-------------------|-----------------|------------------|-----|
| Portland Cement | 4.7 | 63.8 | 2.8 | 2.0 | 0.5 | 2.5 | 21.1 | 2.1 |

TESCAN MIRA 3 scanning electron microscope (SEM) was used in low vacuum and with secondary electron mode to produce the SEM micrograph shown below. SEM micrograph of the Portland cement is shown in Figure 1.

**Figure 1.** SEM micrograph of the OPC.

The water to cement, aggregate to cement and fine aggregate to coarse aggregates ratios of the Ordinary Portland Cement (OPC) were 0.40, 2.50 and 0.75, respectively. The targeted slump of the OPC was 80 mm. The concrete mix design is summarised in Table 2.

Table 2. OPC mix design (kg/m³).

| Cement | Water | Coarse Aggregate | Fine Aggregate |
|--------|-------|------------------|----------------|
| 570 | 228 | 811 | 610 |

Conventional steel bars of 3 mm in diameter with a minimum tensile yield stress of 500 MPa were selected for the steel reinforcements of the concrete pavements. The measured average yield strength of the steel bar was 569 MPa. The steel bars were prepared on the slab formwork with 80 mm spacing along the width of the formwork and 65 mm spacing along the length of the formwork. This is to emulate the typical steel reinforcement bars or mesh that is used in residential and warehouse concrete rigid pavements.

For the fibre reinforced specimens, the fibres used were end-hooked Dramix 3D 65/35BG steel fibres from BOSFA Australia. The properties and geometry of the fibres are summarised in Table 3 below.

Table 3. Property and geometry of the steel fibres.

| Length, <i>l</i> (mm) | Diameter, <i>d</i> (mm) | Aspect Ratio, <i>l/d</i> (mm) | Tensile Strength (N/mm ²) | Young's Modulus (N/mm ²) |
|--------------------------|----------------------------|----------------------------------|--|---|
| 35 | 0.55 | 65 | 1345 | 210,000 |

End-hooked steel fibres were selected due to the increased mechanical anchorage from the addition of the deformed end hook, which further improves the performance of the fibres [22]. The volume fraction of the steel fibres in the fibre reinforced mixes was either 0.5% or 1.0%. For this study, the rigid concrete pavement was produced with either the steel fibres, conventional steel reinforcements or a hybrid of both.

The specimen preparation process started with the drying of aggregates in an oven at 105 °C for at least 24 h to eliminate the moisture content of the aggregates. After 24 h of drying, the aggregates were removed from the oven and stored until the temperature of the aggregates cooled to ambient temperature before casting. This was to ensure consistency between the water added in OPC because additional water had been accounted for during mixing for the additional absorption of the aggregates. A 70 L planetary pan mixer was used to produce the concrete, with the aggregates and cement first added into the pan mixer for 5 min of mixing. This was followed by adding water to the dry mix for an additional 5 min. The characteristic cylinders for compressive and tensile strength testing were poured first because the presence of steel fibres in these cylinders will affect the load path of the cylinders during testing [23]. Therefore, the required dosage of fibres was only added to the fresh concrete mix after the characteristic cylinders were poured. The fibres were added gradually into the fresh concrete mix uniformly to prevent balling for 5 min, with the concrete rigid pavement and crack mouth opening displacement (CMOD) beams poured and compacted subsequently. The CMOD beams were cast as per the methodology recommended in EN 14621 [24]. The slabs that were reinforced with longitudinal reinforcements were cast concurrently with unreinforced slabs to ensure the consistency of the concrete mix. On the next day, the specimens were demoulded and cured in a steam room at 70 °C for 24 h. After accelerated curing, the fatigue specimens were prepared by using an autosaw to cut the concrete slab into prismatic specimens of 50 × 63.5 × 390 mm to reduce the impact of boundary effect from the formwork on the fibre orientation within the specimen.

Specimens produced with steel mesh are denoted with S while specimens produced without the mesh are denoted with M as these specimens only have the OPC matrix. Moreover, 00, 40 and 80 indicates specimens manufactured without fibres, with 0.5% and 1.0% volume fraction of fibres (or 40 kg/m³ and 80 kg/m³). Table 4 below summarises the specimen designations and variables of each batch of slabs produced for this study, with a total of six batches of rigid pavement specimens produced.

Table 4. Summary of the specimens produced.

| Specimens | Fibre Volume Fraction (%) | Fibre Content (kg/m ³) | Steel Bars Addition |
|-----------|---------------------------|------------------------------------|---------------------|
| M-00 | 0.0 | 0.0 | No |
| S-00 | 0.0 | 0.0 | Yes |
| M-40 | 0.5 | 40 | No |
| S-40 | 0.5 | 40 | Yes |
| M-80 | 1.0 | 80 | No |
| S-80 | 1.0 | 80 | Yes |

3. Experimental Program

3.1. Preliminary Fatigue Investigation and Testing

The fatigue testing of the rigid pavement specimens was conducted according to Austroads AG: PT/T233 [25]. An IPC Global servo-pneumatic four-point bending (4PB) testing device was used for this study, as shown in Figure 2.

The 4PB configuration was selected as it eliminates the shear forces on the pavement specimen where a three-point bending testing configuration adds a vertical shear component that increases the crack propagation [26]. Additionally, the 4PB-based testing regime also provided the most comparable

results [27,28]. The 4PB test rig has two end clamps, two loading clamps, a loadcell and a transducer is used. The schematic of the 4PB is presented in Figure 3. The width of the clamps is 25 mm.

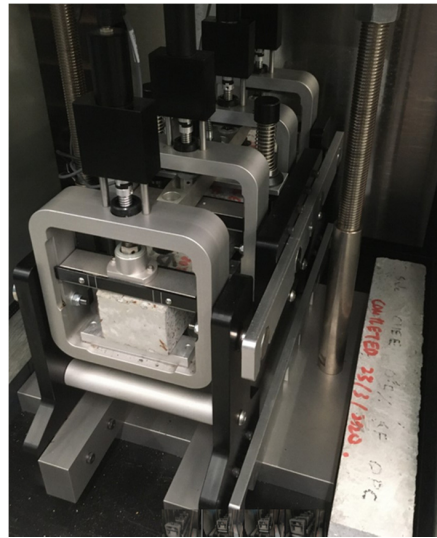


Figure 2. The 4PB testing apparatus in a temperature-controlled cabinet.

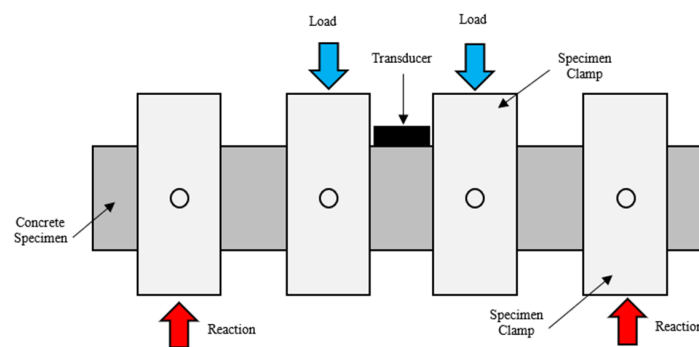


Figure 3. Schematic of the 4PB test from the elevation point of view.

As strain-controlled testing is commonly used for asphalt, strain-controlled testing in haversine sinusoidal load spectra was also adopted for the concrete rigid pavement fatigue life testing, as per the requirements of Austroads AG: PT/T233. The focus of the study is on the fatigue behaviour of warehouse slabs, with the thickness of warehouse slabs typically ranging between 75 and 150 mm, for which a scaled-down rigid pavement is needed [20]. In order to obtain representative results of full-sized pavements, the scaling of the rigid pavement was conducted and complied with [29,30]. The loadings considered were from the movements of forklifts and other light machinery in a typical warehouse, which is 350 kN from each axle. The loading pattern of the forklifts was designated to be 100 to 200 cycles per day as per the Cement Concrete & Aggregate Australia (CCAA) T48 design, construction and specification recommendation [31]. The underlying assumption of the testing regime is that each cycle in the fatigue test is similar to the previous fatigue cycle to enable a consistent testing method to assess the fatigue performance of thick rigid pavements. Therefore, the strain-controlled testing regime would be suitable for thinner concrete elements [1].

Preliminary testing was conducted to identify the most suitable strain loading for the rigid pavement; four strain levels were investigated, which were 75, 123, 140 and 160 microstrains. At lower strain levels of 75 microstrains, it was found that fatigue behaviour was observed, with gradual reduction of the stiffness modulus of the rigid pavement. This indicates that the microcracks were forming in the rigid pavement and fatigue behaviour was occurring. While 75 microstrains may be more representative of a typical loading regime of the application, the rate of the stiffness modulus reduction was slow and resulted in lengthy test duration for each specimen, which is not practical.

The second strain tested was 123 microstrains. The 123 microstrains were calculated based on the cracking moment of the concrete specimens, with the tensile strength data. The cracking moment is defined as the moment (or the force to the lever arm in length) that is needed to cause the concrete to crack on the tension side. This is to take account of the material properties and the geometry of the concrete specimens to provide a systematic method to evaluate thin concrete rigid pavements in high cycle fatigue with the same 4PB test configurations for asphalt. Based on the preliminary testing and mechanics of solids, it was found that 123 microstrains was most appropriate for fatigue testing purposes as it initiates cracking in the concrete at the extreme tensile side in flexural bending. This allowed an opportunity to examine the effectiveness of fibre crack-bridging as fibre bridging can occur after cracking. Moreover, fatigue behaviour with a gradual loss of stiffness modulus was recorded.

On the other hand, strain-controlled at 140 microstrains displayed expected fatigue behaviour in a considerably more rapid degradation than 123 microstrains. However, 140 microstrains strain-controlled was not selected as it is difficult to confirm the mode of the degradation leading to fatigue as the strain level was higher than the cracking strain of the rigid pavement specimens. The 140 microstrains was also 14% higher than the cracking strain of the concrete at 123 microstrains. The fatigue testing regime must be selected carefully to ensure the occurrence of fatigue behaviour, without exerting an excessive amount of permanent deformations on the specimens.

However, at the high 160 microstrains strain level, permanent deformation was believed to occur, with the specimen failing quickly within the first 2000 cycles. This is due to the formation of macrocracks from the excessive strain applied, and the data obtained from the concrete pavement showed low cycle fatigue. The behaviour observed in the preliminary study was expected due to the rigidity of concrete. Thus, this indicated that higher strain levels were not suitable. The strain behaviour observed in this study is consistent with Melese et al.'s (2020) work [6], where there was a range of suitable strain levels for fatigue testing of asphalt at 4PB. However, concrete has a narrower range of strains for testing in comparison to asphalt as the material is comparably less flexible compared to asphalt. Hence, 123 microstrains were selected as the strain level used for the fatigue test of concrete rigid pavement at 4PB configuration. Figure 4 below summarises the findings of the preliminary testing.

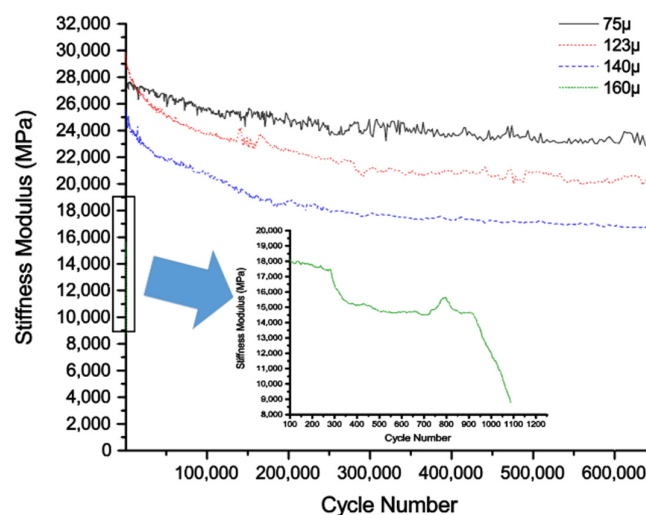


Figure 4. Trial test of rigid pavement at 75 microstrains, 123 microstrains, 140 microstrains and 160 microstrains.

Di Benedetto et al. (2004) suggested that it is crucial to select the most suitable loading level to ensure that the fatigue degradation process is occurring in the fatigue tests, for which 123 microstrains was selected [28]. The 123 microstrains were also selected to comply with the requirement of the Austroads AG: PT/T233 standard for an accelerated fatigue testing methodology that is practical in industry applications.

Prior to testing, the concrete prisms were stored in a temperature-controlled cabinet for at least 3 h to allow the temperature of the specimens to be 20 °C to eliminate the temperature effect. The initial stiffness modulus was collected at 100 cycles as concrete tends to have a steeper initial decline than asphalt. Frequency of strain applied was set at 10 Hz as typical traffic frequency is between 3 and 16 Hz [32]. CCAA T48 also has provisions on the maximum speed of forklifts to be 25 km/h, which is around 10 Hz for a typical forklift wheelbase. However, due to the lengthy nature of fatigue testing, the cycle limit of the test has to be limited to 1 million to ensure the practicality of the experimental work. Additionally, to ensure compliance with the Austroads AG: PT/T233 standard, the termination condition of the fatigue testing was either at one million cycles or a reduction of stiffness modulus by 50% [25]. At least 5 rigid concrete pavement beams were tested for each variable in this study.

3.2. Absorption

The absorption or apparent volume of permeable voids (AVPV) of the fatigue specimens was conducted according to AS 1012.21:1999 (R2014) [33]. The AVPV test was conducted to determine the changes in voids for the specimens to determine the effectiveness of different types of reinforcements in terms of crack control in the thin rigid concrete pavements. The absorption of the fatigue specimens was collected before and after the 4PB fatigue test to determine the formation of microcracks or the change in permeable voids in the concrete matrix of the specimens tested. The formation of microcracks has a profound influence on the fatigue life of the rigid pavement as the excessive formation of microcracks in rigid pavements would result in poor fatigue life with macrocracks appearing. Therefore, the absorption test was conducted to quantify the increase in microcracks of concrete.

3.3. Compressive and Indirect Tensile Strength

The concrete unconfined compressive strength was measured according to AS 1012.9:2014 [34] at 20 MPa/min loading rate on a Universal Testing Machine (UTM). This is to quantify the capacity of the concrete in compression. Data on the indirect tensile strength were collected as per AS 1012.10:2000 (R2014) to quantify the tensile capacity of the concrete produced [35].

3.4. Crack Mouth Opening Displacement (CMOD)

The residual tensile strength of the fibres was obtained via the CMOD test by EN 14,651 [24], to quantify the tensile capacity of fibres after the concrete was fully cracked. The test was chosen to investigate the performance of the end-hooked fibres at 0.5% and 1.0% volume fractions. The 150 × 150 × 550 mm beams were cast and notched before the test. A UTM with 300 kN capacity was used to obtain the residual tensile strength, with a crack mouth displacement gauge.

4. Results and Discussion

4.1. Material Properties

The results of the average compressive strength, tensile strength and CMOD are summarised in Table 5.

Table 5. Average compressive strength, tensile strength and residual tensile strength of the OPC concrete.

| Fibre Volume Fraction | Compressive Strength (MPa) | | Tensile Strength (MPa) | Residual Tensile Strength (MPa) | | | | |
|-----------------------|----------------------------|--------|------------------------|---------------------------------|----------|----------|----------|-------|
| | f_{cm} | f'_c | f_{ct} | f_{R1} | f_{R2} | f_{R3} | f_{R4} | f_w |
| 0.0% | 63.1 | 53.8 | 4.2 | Not Applicable | | | | |
| 0.5% | 61.9 | 52.7 | 4.4 | 4.8 | 6.2 | 5.9 | 5.4 | 1.3 |
| 1.0% | 58.1 | 49.2 | 4.6 | 5.5 | 10.6 | 9.5 | 7.5 | 2.3 |

The concrete properties were found to be sufficiently consistent for the comparison between different fibre dosages. The residual tensile strength of the fibre reinforced concrete was found to be 1.3 MPa for 0.5% volume fraction and 2.3 MPa for 1.0% volume fraction.

4.2. Fatigue Testing

With the raw data collected from the 4PB test rig, the following equations were used to calculate the tensile stress, tensile strain and flexural modulus with Equations (1)–(3) below [25]. The calculations were computed based on the maximum force at the amplitude and the deflection at mid-span of the rigid pavement specimen.

$$\sigma = 0.36 \times \frac{P}{bh^2} \quad (1)$$

$$\varepsilon = \frac{12\delta h}{3L^2 - 4a^2} \quad (2)$$

$$S = \frac{\sigma}{\varepsilon} \quad (3)$$

where σ is peak tensile flexural stress; P is peak force exerted on the pavement specimen; b is the width of the specimen; h is the height of the specimen; ε is peak tensile strain; δ is maximum deformation at midspan of the pavement specimen; L is the distance between the 4PB loading frame's outer clamps; a is distance between the 4PB loading frame's inner clamps; S is the stiffness modulus of the pavement specimen.

For each batch of specimens tested in fatigue at each reinforcement level, Chauvenet's criterion was applied to remove outliers from the dataset, as per the methodology by Singh et al. (2007) [13]. The averages of fatigue cycles, percentage of stiffness modulus lost and phase angles at first 100 cycles and termination are listed in Table 6.

Table 6. Averages of stiffness modulus, dissipated energy and phase angle from fatigue tests.

| | Fatigue Cycles | Stiffness Loss (%) | Phase Angle at 100 Cycle (°) | Phase Angle at Termination (°) |
|------|----------------|--------------------|------------------------------|--------------------------------|
| M-00 | 151,100 | 50 | 0.73 | 1.53 |
| S-00 | 306,800 | 50 | 0.54 | 2.08 |
| M-40 | 355,600 | 48 | 0.40 | 1.95 |
| S-40 | 604,000 | 39 | 0.63 | 1.47 |
| M-80 | 603,000 | 46 | 0.80 | 1.42 |
| S-80 | 667,600 | 40 | 0.82 | 1.82 |

For a visual representation, Figure 5 shows the changes in stiffness modulus at initial 10 cycles and at termination.

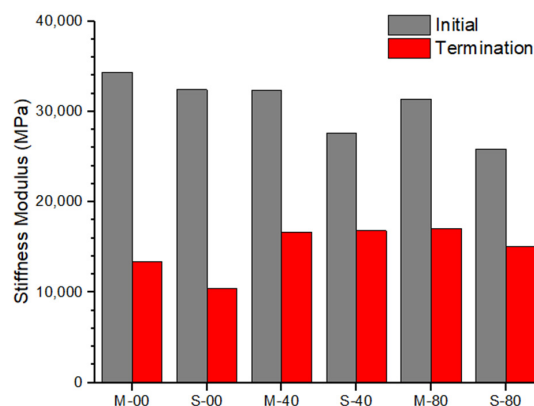


Figure 5. Stiffness modulus of the rigid pavement specimens at the start and the end of the 4PB fatigue tests.

Figures 6 and 7 shows the average fatigue cycles and average stiffness modulus loss of five specimens. Figure 8 demonstrates the changes in phase angles at the beginning and at the termination of the fatigue test.

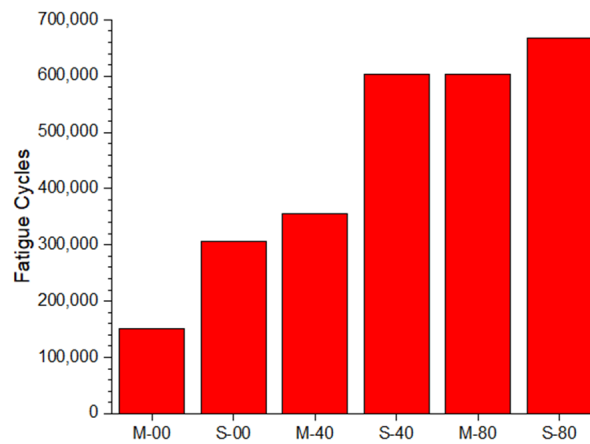


Figure 6. Average number of fatigue cycles to the end of the 4PB fatigue tests at either 50% stiffness modulus lost or 1 million cycles limit.

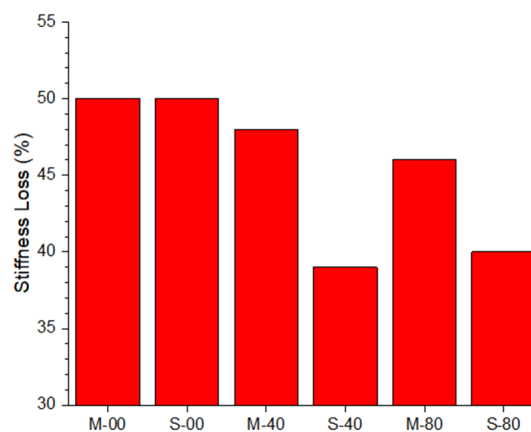


Figure 7. Stiffness loss of rigid pavement specimens tested in 4PB fatigue tests.

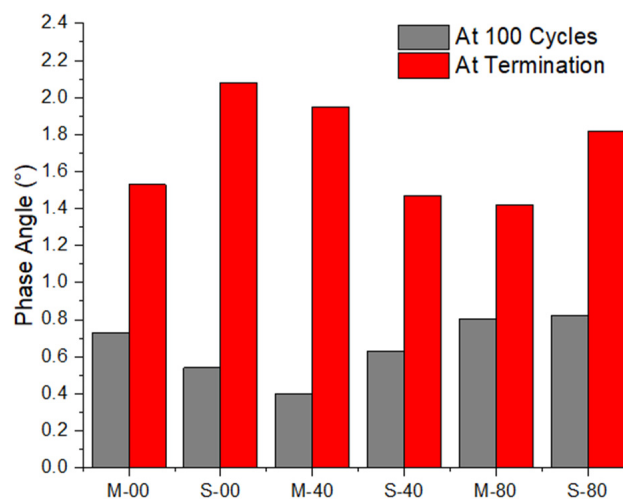


Figure 8. Average phase angle at first 100 cycles and termination of rigid pavement specimens tested in 4PB fatigue tests.

The reduction of stiffness modulus occurred due to the reduction of peak force, P , as the fatigue test is conducted as strain is maintained constant throughout the fatigue test. Figure 9 demonstrates the typical stress–strain relationship of the beams tested.

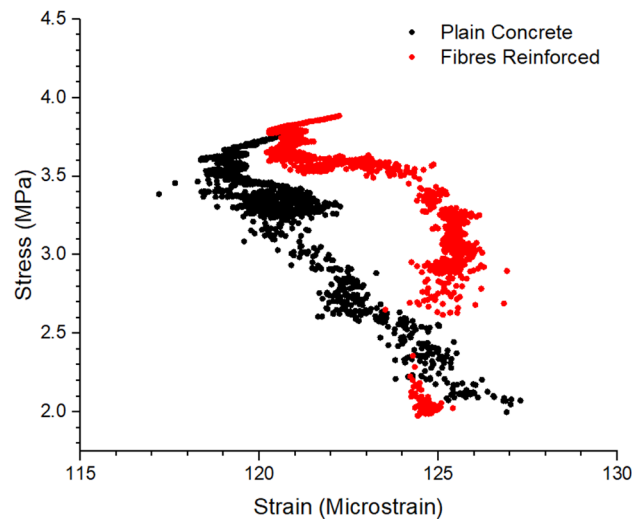


Figure 9. Typical stress–strain curves of plain concrete (200,200 cycles fatigue life) and fibre reinforced concrete (624,100 cycles fatigue life).

The degradation of plain concrete demonstrates a steep decline in stress compared to fibre reinforced specimens. The stress decline of fibre reinforced beams was found to be more gradual initially. The failure of the fibre reinforced beams was steeper towards termination but the fibre’s crack-bridging prevented it from brittleness and rapid failure to termination.

It was found that the fatigue cycles of the specimens tested at cracking strain were on average 151,100 to 667,600 for the rigid pavement specimens tested. However, it is important to note that rigid concrete pavements that consisted of high fibre volume fractions reached the 1 million termination condition. Hence, the number of cycles of the concrete rigid pavements was considered as high-cycle fatigue, as per Model Code 2010 [36]. It is important to state that the rigid pavement beams tested were found to have no visible macrocracks formed after the fatigue test.

The unreinforced concrete specimens, M-00 series, has the lowest fatigue life among the six variables tested in this study, with an average of 151,100 cycles recorded for the termination of the 4PB fatigue test. The average stiffness loss of the M-00 batch was 50%, with all rigid pavement specimens terminated at 50% stiffness modulus reduction. On the other hand, the rigid pavement specimens with longitudinal reinforcements, S-00 series, were found to have their fatigue life doubled to 306,800 cycles, which showed that the presence of reinforcements able to improve the fatigue cycles. Similar to the M-00, the S-00 specimens with longitudinal reinforcements had an average termination stiffness of 50%. The phase angles of the M-00 and S-00 specimens were recorded to be largely similar values of 0.73° and 0.54° at the first 100 cycles, with the phase angles increasing to 1.53° and 2.08° at termination. This illustrates that the concrete material behaved elastically, in comparison to asphalt, as the lag in time between applied load and resultant strain was close to 0° [37]. However, the increase in phase angle was observed towards the conclusion of the 4PB test; this indicates that macrocracks have been formed, with a significant reduction in stiffness of the rigid pavement specimens. The non-fibre reinforced rigid pavement specimens were designated as reference specimens to the fibre reinforced specimens in this study.

With 0.5% volume fraction of fibres added into the concrete matrix, the M-40 specimens were found to have an average of 355,600 fatigue cycles. The use of 0.5% volume fraction of fibres in the M-40 batch led to an average 135% increase over plain concrete rigid pavements (M-00 series). Moreover, it was found a relatively marginal 15% increase in fatigue life cycle over the specimens manufactured

in plain concrete with longitudinal bars (S-00 series). The stiffness loss of the M-40 specimens was observed to dropped slightly to 48% on average. Further improvements in fatigue were able to be achieved with the composite application of 0.5% fibre volume fraction with steel reinforcements in the S-40 specimens. Similar to S-00, S-40 specimens have a higher fatigue life span, with an average of 604,000 fatigue cycles. Three S-40 specimens were able to reach the 1,000,000 cycles termination condition. The increase in fatigue cycles was found to be nearly 300% and 200% increase to the M-00 and S-00 series. The phase angle of both M-40 and S-40 specimens was observed to be largely similar to the non-fibre reinforced specimens in this study, with phase angles found to be 0.60° and 0.63° , respectively. The phase angle of both variables was found to increase to 1.95° and 1.47° for M-40 and S-40 after the fatigue test, and a similar trend was recorded in phase angles as M-00 and S-00. The stiffness loss was further decreased to 39%. The findings provide strong evidence of the benefits of the application of fibre reinforced concrete in steel reinforcement composites to improve the fatigue life of concrete structures.

The fatigue life of the M-80 specimens was recorded to be 603,000 cycles, with around 200% to 300% increase in fatigue life to M-00 and S-00. Moreover, the fatigue life of the M-80 specimens was similar to S-40, which suggests that 1.0% addition of fibres offers similar performance to concrete rigid pavements that were longitudinal steel reinforced with 0.5% fibre volume fraction in the fibre matrix. However, the average stiffness loss was higher than S-40 specimens as the M-80 specimens recorded a 46% average stiffness loss. This suggests that longitudinal steel bars still have a significant positive effect on fatigue in rigid concrete pavements. The 1.0% fibre addition into concrete rigid pavements reinforced with longitudinal steel (S-80) was found to have the highest fatigue life in this study. S-80 was recorded to have 667,600 cycles to termination, with the lowest stiffness loss at 40%, where it was indicative that hybrid steel bars and fibres, S-80, offered the most optimal fatigue performance in this study. The increase in fatigue life in S-80 was found to be comparably marginal fatigue improvement over M-80, with 10% higher fatigue cycles and 15% lower stiffness losses to M-80. The phase angles of M-80 and S-80 were 1.01° and 0.83° at the first 100 cycles, respectively, that was higher than the unreinforced and 0.5% volume fraction specimens. At the end of the fatigue test, the average phase angle increased to 1.42° and 1.82° for M-80 and S-80. It is believed that the increased fibre content may lead to a reduction in elasticity but the phase angles of the 1.0% fibre volume fraction specimens were still comparably lower than most asphalt pavements [6,37,38].

4.3. Energy Dissipation

The fatigue damage of concrete was evaluated through the concept of energy, where part of the work energy from the 4PB exerted on the specimens under flexural is converted into heat and the other part of the work energy remains as the internal energy stored in the specimen [2]. The elastic deformation of pavement under flexural bending is known to be recoverable but some of the energy such as fracture energy and heat is dissipated from the system. The dissipated energy of each cycle is denoted as the changes in the area of each hysteresis loop of the stress–strain graphs of the pavement specimens under flexural bending. Hence, the cumulative energy dissipation of the specimens tested in fatigue is calculated by Guzman and Carpenter's (2000) equation [39]. The dissipated energy of each cycle and cumulative dissipated energy to n cycle of each specimen were calculated based on Equations (4)–(6), and the average energy dissipated of each variable is presented in Table 7.

$$\phi = 320 fs \quad (4)$$

$$W_i = \pi \sigma \epsilon \sin \phi \quad (5)$$

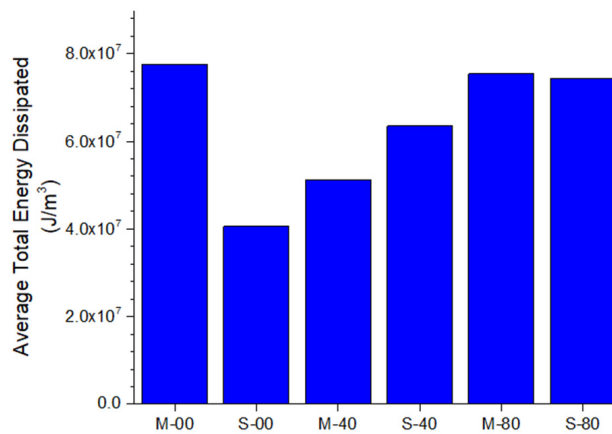
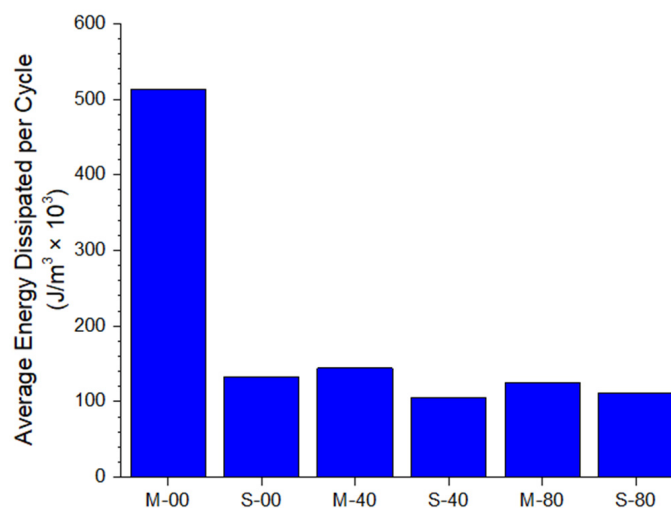
$$W_t = \sum_{i=1}^n W_i \quad (6)$$

where W_i is the dissipated energy at each cycle; ϕ is the phase angle of each cycle; W_t is the total dissipated energy of the fatigue test; f is the frequency of the load exerted; s is the time lag between load at midspan and the deflection at midspan is recorded.

Table 7. Averages of total dissipated energy and dissipated energy per cycle from fatigue tests.

| | Average Total Dissipated Energy (J/m ³) | Fatigue Cycles | Average Energy Dissipated per Cycle (J/m ³ × 10 ³) |
|------|---|----------------|---|
| M-00 | 77,478,400 | 151,100 | 513 |
| S-00 | 40,585,200 | 306,800 | 132 |
| M-40 | 51,259,300 | 355,600 | 144 |
| S-40 | 63,446,300 | 604,000 | 105 |
| M-80 | 75,375,200 | 603,000 | 125 |
| S-80 | 74,340,300 | 667,600 | 111 |

Table 7 summarises the calculated averages of total dissipated energy and energy dissipated per cycle, and the values obtained are plotted in Figures 10 and 11.

**Figure 10.** Total energy dissipated of the concrete specimens tested.**Figure 11.** The energy dissipated per cycle of the concrete specimens tested.

The total dissipated energy represents the sum of the energy emitted from the rigid pavement throughout the 4PB fatigue testing. On the other hand, the energy dissipated per cycle was obtained by averaging the total dissipated energy with the numbers of cycles of the fatigue test prior to termination. It was found that the use of energy dissipated per cycle would be a more representative comparison of reinforced and unreinforced thin rigid concrete pavements over total energy dissipated.

The M-00 specimens had the highest total dissipated energy and energy dissipated per cycle in the study, at 77,478,400 J/m³ in total and average 513 J/m³ per cycle. The lack of reinforcements providing tensile resistance in M-00 led to the highest energy dissipation in each cycle for the unreinforced specimens. It is believed that this is the reason that unreinforced pavement specimens failed rapidly, with lower fatigue cycles compared to the reinforced specimens in this study. This can be explained by the fact that the concrete was fully cracked at the first few cycles in 4PB. Then, the concrete could not provide sufficient flexural tensile strength due to the reduction in the effective depth of the section from the cracks extending into the section. This led to lower section modulus value that reduces the load applied to maintain the constant strain as the fatigue test was conducted with strain-controlled testing. Hence, it is believed that a relatively significant amount of microcracks was formed in unreinforced rigid pavement specimens in each cycle compared to reinforced specimens that led to the highest value in energy dissipated per cycle in this study.

With the addition of reinforcements to the concrete matrix, the total energy dissipated was noted to have an increasing trend to the increase in fibre volume fraction and on the presence of steel reinforcements. The unreinforced concrete matrix that was reinforced with longitudinal steel (S-00) was recorded to have an average total dissipated energy of 40,585,200 J/m³, which is the lowest among the reinforced specimens. For the 0.5% fibre volume fraction specimens, M-40 and S-40 specimens showed an increasing amount of total dissipated energy, with the total dissipated energy calculated as 51,259,250 J/m³ and 63,446,250 J/m³ throughout the entire fatigue test conducted. Finally, the M-80 and S-80 specimens with 1.0% fibre volume fractions were found to have 75,375,200 J/m³ and 74,340,333 J/m³ of total dissipated energy.

It was also noted that a different trend was observed with the reinforced specimens of either steel bars, fibres or hybrid of both in terms of energy dissipated per cycle, with energy dissipated per cycle of S-00 reduced to an average of 132 J/m³ per cycle. In comparison to the completely unreinforced M-00 specimens, the specimens produced with only longitudinal bars in the unreinforced concrete matrix were shown to have a significant reduction in average energy dissipated in each cycle. However, the addition of steel fibres into the concrete matrix also led to a further reduction in the average energy dissipation in each cycle of fatigue testing. The pure steel fibre reinforced M-40 and M-80 were able to reduce the average cyclic energy dissipation to 144 J/m³ per cycle and 125 J/m³ per cycle, respectively. With 0.5% and 1.0% volume fraction in longitudinally reinforced pavement specimens, the energy dissipated per cycle further declined to an average of 105 J/m³ per cycle and 111 J/m³ per cycle. Based on the results of this study, the hybrid reinforced thin rigid concrete pavements were able to provide the most optimal fatigue performance. It is known that the heat energy dissipation and fracture energy of material under fatigue loading is generally constant [2,40], but the observations found in this study suggest that the energy dissipation from damage is not constant as the type of reinforcement used and fibre dosage has a noticeable effect on the dissipated energy from fracture.

4.4. Apparent Volume of Permeable Voids (AVPV)

The AVPV of the fatigue concrete specimens were collected prior and after the 4PB fatigue loading. This was done to examine the effect of fibres and longitudinal reinforcements on the changes in the permeable voids in the concrete matrix as the crack bridging of steel fibres can reduce microcracks formation. Subsequently, the changes in permeable voids were calculated, with the findings summarised in Table 8 and Figure 12 below.

Table 8. AVPV of the concrete specimens measured before 4PB, after 4PB and the changes in AVPV.

| | M-00 | S-00 | M-40 | S-40 | M-80 | S-80 |
|---------------------|------|------|------|------|------|------|
| Before 4PB (%) | 10.7 | 11.0 | 12.8 | 13.0 | 11.2 | 11.9 |
| After 4PB (%) | 12.8 | 13.1 | 14.2 | 14.1 | 12.5 | 13.1 |
| Changes in AVPV (%) | 2.1 | 2.1 | 1.3 | 1.1 | 1.3 | 1.2 |

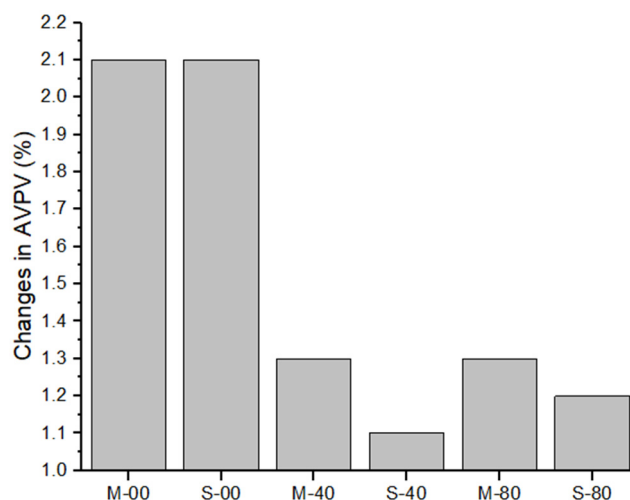


Figure 12. Changes in the AVPV of the concrete specimens.

Based on Table 8, the AVPV of the rigid pavements tested did not vary significantly before 4PB fatigue loading. However, the changes in permeable voids were noted to be noticeable after the 4PB fatigue test. Specimens with a purely concrete matrix were found to have higher percentages of increase in permeable voids in the concrete matrix compared to fibre reinforced specimens. The M-00 and S-00 specimens both have approximately 2.1% more permeable voids formed after the 4PB testing. The fibre reinforced concrete specimens (M-40 and M-80) were found to have a decrease in permeable voids formed post 4PB loading at 1.3%. The results obtained support the notion that the addition of fibres to concrete can reduce the number of cracks formed due to the crack bridging mechanism provided by the fibres. Subsequently, the use of longitudinal reinforcements in fibre reinforced rigid pavement was able to introduce a further reduction to 1.1% to 1.2% in the permeable voids formed in post 4PB testing. Thus, the results found were supportive of the application of hybrid reinforced concrete rigid pavements, with steel fibres and longitudinal bars capable of providing more optimal fatigue performance with the observations obtained via 4PB fatigue testing. This also provides further evidence that the addition of steel fibres is able to reduce microcrack formations.

5. Discussion and Analysis of the Results

Referring to the 4PB fatigue tests and the AVPV measurements obtained in this study, it is noted that the application of longitudinal steel bars and steel fibres was able to significantly improve the fatigue performance of thin rigid pavements. The methodology derived in this study can demonstrate a clear trend in the fatigue behaviour of thin rigid pavements with different combinations of reinforcements. This suggests that the strain level selected is suitable for examining the fatigue behaviour of both reinforced and unreinforced concrete.

The addition of steel fibres in the concrete matrix can provide some tensile capacity in the pavements that are under flexural bending, with the effective 3D network of overlapped fibres enabling the crack bridging when cracks are formed in concrete under flexural bending. Poveda et al. (2017) mentioned that the presence of fibres in the concrete matrix that is under fatigue loading is able to control microcracking and delay the formation of macro cracks [14]. Meanwhile, it can also be explained that the poor concrete tensile capacity is the reason that the plain concrete specimens have the lowest fatigue life, highest average energy dissipation per cycle and highest stiffness loss of all the concrete rigid pavement specimens tested in this study [21]. The results obtained are also in agreement from the perspective of energy dissipation in this study, with significantly lower average dissipated energy per cycle observed in fibre reinforced specimens in comparison to the plain concrete ones. Moreover, the findings in this study are in agreement with Song et al.'s work [1]. Therefore, the rigid pavement specimens reinforced with only steel fibres at 0.5% and 1.0% steel volume fraction were able

to demonstrate higher fatigue life compared to the plain concrete specimens. The reduction of the average energy dissipated per cycle occurred due to increased fibre dosage, where the higher dosage of fibres was able to reduce the possibility of cracks in fibres to nucleate and propagate through the concrete matrix that is the least reinforced [41,42]. This is reflected by the results on the fatigue life of 1.0% volume fractions, which are higher than rigid concrete specimens with 0.5% volume fractions. This is because the cracks in fibre reinforced concrete tend to propagate through the path of least resistance in concrete mixes that have a relatively low volume fraction of fibres [43].

With the inclusion of the longitudinal steel in the specimens under flexural fatigue bending, the fatigue life of those pavements was observed to be improved over the purely fibre reinforced matrix. The longitudinal bars provide the balancing tension force to the compressive stress block at the top of the specimen, which produces a coupling force to reduce the microcrack formation on the tension side and increased the fatigue life. It is also hypothesised that tension stiffening may also have an impact on the improved fatigue performance of steel bar reinforced concrete specimens compared to plain concrete specimens. The addition of fibres leads to further improvements in fatigue life when fibres are added compositely with longitudinal reinforcements in concrete pavements. The presence of steel fibres in the concrete matrix is able to contribute by taking some of the tensile stresses applied on the pavement and also reducing the stresses in the longitudinal bars in the concrete pavement [15,44]. Additionally, the hybrid reinforced pavements with both fibres and steel bars were able to decrease the crack width and reduce the strain of the steel bars due to the crack bridging effect of fibres [15]. Thus, the composite reinforcements of rigid concrete pavement slabs reduced the stress exerted on the steel bars, which led to fewer microcracks produced and improved fatigue performance of concrete pavements. In terms of the energy dissipation perspective, hybrid reinforced concrete pavements are able to further decrease the average energy dissipation of concrete in each cycle, and increases in fatigue life span and lower changes in permeable voids were achieved. This will result in higher numbers of fatigue cycles in hybrid reinforced rigid pavements that are constructed with steel fibres and bars. Hence, the longer service life of the compositely reinforced pavement is achievable with the application of both fibres and steel reinforcements.

6. Conclusions

The observations in this study were found to demonstrate the varying fatigue behaviour of concrete rigid pavements with either fibres only, longitudinal steel bars only or a combination of both. The conclusions are summarised below:

1. The scaled-down, strain-based approach to 4PB fatigue testing of rigid pavements is deemed to be suitable as it demonstrated the behaviour of both reinforced and unreinforced concrete pavements under fatigue. The methodology proposed is suitable to assess the fatigue performance of both plain concrete and fibre reinforced concrete thin pavements. The fatigue life of the concrete pavements correlates with the energy dissipation obtained in this study with the data collected on the various specimens in this study.
2. Hybrid reinforcement of both steel fibres and steel reinforcements were found to be the most optimal reinforcement to maximise the service life of concrete rigid pavements in fatigue loading. This is due to the tensile stresses of specimens loaded in cyclic flexural able to be redistributed between the steel fibres and steel reinforcement to reduce the formation of microcracks. Therefore, this further reduced the loss of stiffness modulus and increase fatigue cycles.
3. The fracture energy in the total energy dissipated does not remain constant for a different combination of reinforcements applied in the concrete pavements. The addition of steel fibres, longitudinal steel or both has an impact on the energy dissipated in each cycle of concrete specimens under fatigue testing. Hybrid reinforced specimens with both fibres and bars have the lowest energy dissipation per cycle.
4. In comparison to plain concrete, the use of steel fibres without conventional reinforcements in concrete rigid pavement were also shown to have significant improvements in the fatigue

resistance of the pavements. The addition of steel fibres in concrete pavements has resulted in at least a 135% increase in fatigue cycles compared to the fatigue cycles of plain concrete. This demonstrates the effectiveness of fibres in plain concrete under fatigue as fibres provide crack bridging to control the cracks formed.

Author Contributions: Conceptualisation, T.N.S.H.; methodology, T.N.S.H. and C.K.L.; validation, T.N.S.H. and C.K.L.; formal analysis, C.K.L.; investigation, C.K.L.; resources, T.N.S.H., A.C. and H.N.; data curation, C.K.L.; writing—original draft preparation, T.N.S.H. and C.K.L.; writing—review and editing, T.N.S.H., C.K.L, A.C. and H.N.; visualisation, C.K.L.; supervision, T.N.S.H. and A.C.; project administration, T.N.S.H. and A.C. All authors have read and agreed to the published version of the manuscript.

Funding: This research received no external funding.

Acknowledgments: The authors would like to thank and acknowledge BOSFA Australia for providing the 65/35BG 3D fibres used in this study. Part of this research was undertaken using the electron microscopy instrumentation (ARC LE130100053) at the John de Laeter Centre, Curtin University. The authors are grateful for the assistance from Jaehoon Kim, Darren Isaac, Mark Whittaker and Elaine Miller. The corresponding first author is appreciative of the support provided by the Australian Government through the Australian Government Research Training Program (RTP) initiative.

Conflicts of Interest: The authors declare no conflict of interest.

References

1. Song, Z.; Frühwirt, T.; Konietzky, H. Characteristics of dissipated energy of concrete subjected to cyclic loading. *Constr. Build. Mater.* **2018**, *168*, 47–60. [CrossRef]
2. Lei, D.; Zhang, P.; He, J.; Bai, P.; Zhu, F. Fatigue life prediction method of concrete based on energy dissipation. *Constr. Build. Mater.* **2017**, *145*, 419–425. [CrossRef]
3. Al-rkaby, A.H.J.; Chegenizadeh, A.; Nikraz, H.R. Cyclic behavior of reinforced sand under principal stress rotation. *J. Rock Mech. Geotech. Eng.* **2017**, *9*, 585–598. [CrossRef]
4. Lee, Y.-L.; Barkey, M.E.; Kang, H.-T. *Metal Fatigue Analysis Handbook: Practical Problem-Solving Techniques for Computer-Aided Engineering*; Elsevier: Amsterdam, The Netherlands, 2011.
5. Zou, X.; Ding, B.; Peng, Z.; Li, H. Damage analysis four-point bending fatigue tests on stone matrix asphalt using dissipated energy approaches. *Int. J. Fatigue* **2020**, *133*, 105453. [CrossRef]
6. Melese, E.; Baaj, H.; Tighe, S. Fatigue behaviour of reclaimed pavement materials treated with cementitious binders. *Constr. Build. Mater.* **2020**, *249*, 118565. [CrossRef]
7. Mohod, M.V.; Kadam, K. A comparative study on rigid and flexible pavement: A review. *IOSR J. Mech. Civ. Eng.* **2016**, *13*, 84–88.
8. Wang, H.; Yang, J.; Lu, G.; Liu, X. Accelerated Healing in Asphalt Concrete via Laboratory Microwave Heating. *J. Test. Eval.* **2020**, *48*, 739–757. [CrossRef]
9. Löfgren, I. Fibre-Reinforced Concrete for Industrial Construction. Ph.D. Thesis, Chalmers University of Technology, Göteborg, Sweden, 2005. Available online: <https://core.ac.uk/download/pdf/70560762.pdf> (accessed on 11 September 2020).
10. Chegenizadeh, A.; Keramatikerman, M.; Nikraz, H. Liquefaction resistance of fibre reinforced low-plasticity silt. *Soil Dyn. Earthq. Eng.* **2018**, *104*, 372–377. [CrossRef]
11. Ng, T.S.; Htut, T.N.S. Steel Fibre Concrete Pavements: Thinner And More Durable. *Concr. Aust.* **2018**, *44*, 44–51.
12. Ng, T.S.; Htut, T. Structural application of steel fibre reinforced concrete with and without conventional reinforcement. In Proceedings of the Australian Structural Engineering Conference: ASEC 2018, Adelaide, Australia, 25–28 September 2018; p. 624.
13. Singh, S.P.; Mohammadi, Y.; Goel, S.; Kaushik, S.K. Prediction of Mean and Design Fatigue Lives of Steel Fibrous Concrete Beams in Flexure. *Adv. Struct. Eng.* **2007**, *10*, 25–36. [CrossRef]
14. Poveda, E.; Ruiz, G.; Cifuentes, H.; Yu, R.C.; Zhang, X. Influence of the fiber content on the compressive low-cycle fatigue behavior of self-compacting SFRC. *Int. J. Fatigue* **2017**, *101*, 9–17. [CrossRef]
15. Parvez, A.; Foster, S.J. Fatigue of steel-fibre-reinforced concrete prestressed railway sleepers. *Eng. Struct.* **2017**, *141*, 241–250. [CrossRef]

16. Chen, M.; Zhong, H.; Zhang, M. Flexural fatigue behaviour of recycled tyre polymer fibre reinforced concrete. *Cem. Concr. Compos.* **2020**, *105*, 103441. [CrossRef]
17. Pasetto, M.; Baldo, N. Dissipated energy analysis of four-point bending test on asphalt concretes made with steel slag and RAP. *Int. J. Pavement Res. Technol.* **2017**, *10*, 446–453. [CrossRef]
18. Artamendi, I.; Khalid, H. Characterization of fatigue damage for paving asphaltic materials. *Fatigue Fract. Eng. Mater. Struct.* **2005**, *28*, 1113–1118. [CrossRef]
19. Jamadin, A.; Ibrahim, Z.; Jumaat, M.Z.; Hosen, M.A. Serviceability assessment of fatigued reinforced concrete structures using a dynamic response technique. *J. Mater. Res. Technol.* **2020**, *9*, 4450–4458. [CrossRef]
20. Standards Australia. AS 3727.1:2016—Pavements Part 1: Residential. 2016. Available online: <https://www-saiglobal.com.dbgw.lis.curtin.edu.au/online/Script/OpenDoc.asp?name=AS+3727%2E1%3A2016&path=https%3A%2F%2Fwww%2Esaiglobal%2Ecom%2FPDFTemp%2Fosu%2D2020%2D09%2D29%2F8739766302%2F3727%2E1%2D2016%2Epdf&docn=EPCO6318674045> (accessed on 5 June 2019).
21. Chalioris, C.E.; Karayannis, C.G. Effectiveness of the use of steel fibres on the torsional behaviour of flanged concrete beams. *Cem. Concr. Compos.* **2009**, *31*, 331–341. [CrossRef]
22. Abdallah, S.; Fan, M.; Cashell, K.A. Pull-out behaviour of straight and hooked-end steel fibres under elevated temperatures. *Cem. Concr. Res.* **2017**, *95*, 132–140. [CrossRef]
23. Olesen, J.F.; Østergaard, L.; Stang, H. Nonlinear fracture mechanics and plasticity of the split cylinder test. *Mater. Struct.* **2006**, *39*, 421–432. [CrossRef]
24. European Committee for Standardization. *Test Method for Metallic Fibered Concrete—Measuring the Flexural Tensile Strength (Limit of Proportionality (Lop), Residual)*; BSI Standards: London, UK, 2005.
25. AG:PT/T233 Fatigue Life of Compacted Bituminous Mixes Subject to Repeated Flexural Bending. 2006. Available online: <https://austroads.com.au/publications/pavement/agpt-t233-06> (accessed on 3 April 2019).
26. Pronk, A.C. Theory of The Four Point Dynamic Bending Test Part I: General Theory. 2007. Available online: <http://www.civil.uminho.pt/4pb/information/theory/4PB-I-General.pdf> (accessed on 17 May 2020).
27. Arsenie, I.M.; Chazallon, C.; Duchez, J.-L.; Hornych, P. Laboratory characterisation of the fatigue behaviour of a glass fibre grid-reinforced asphalt concrete using 4PB tests. *Road Mater. Pavement Des.* **2017**, *18*, 168–180. [CrossRef]
28. Di Benedetto, H.; de La Roche, C.; Baaj, H.; Pronk, A.; Lundström, R. Fatigue of bituminous mixtures. *Mater. Struct.* **2004**, *37*, 202–216. [CrossRef]
29. Mier, J.G.M.V. *Concrete Fracture: A Multiscale Approach*; CRC Press: Boca Raton, FL, USA, 2013.
30. Mier, J.G.M.V. *Fracture Processes of Concrete: Assesments of Material Parameter for Fracture Models*; CRC Press: Boca Raton, FL, USA, 1997.
31. Cement Concrete & Aggregates Australia. CCAA T48—Guide to Industrial Floors and Pavements—Design, Construction and Specification; Cement Concrete & Aggregates Australia: Sydney, Australia, 2009.
32. Gettu, S.J.S.R. Fatigue fracture of fibre reinforced concrete in flexure. *Mater. Struct.* **2020**, *53*, 56.
33. Standards Australia. AS 1012.21:1999 (R2014)-Methods of Testing Concrete—Determination of Water Absorption and Apparent Volume of Permeable Voids in Hardened Concrete; Standards Australia: Sydney, Australia, 1999.
34. Standards Australia. AS 1012.9:2014-Methods of Testing Concrete—Method 9: Compressive Strength Tests—Concrete, Mortar and Grout Specimens; Standards Australia: Sydney, Australia, 2014.
35. Standards Australia. *Methods of Testing Concrete Determination of Indirect Tensile Strength of Concrete Cylinders Saiglobal (as 1012.10-2000 (r2014))*; Standards Australia: Sydney, Australia, 2014.
36. Taerwe, L.; Matthys, S.; New Model Code Fib Special Activity Group. *Fib Model Code for Concrete Structures 2010*; Ernst & Sohn, Wiley: Hoboken, NJ, USA, 2010; pp. I–XXXIII. [CrossRef]
37. Naik, A.K.; Biligiri, K.P. Predictive Models to Estimate Phase Angle of Asphalt Mixtures. *J. Mater. Civ. Eng.* **2015**, *27*, 04014235. [CrossRef]
38. Brovelli, C.; Crispino, M.; Pais, J.C.; Pereira, P.A.A. Assessment of Fatigue Resistance of Additivated Asphalt Concrete Incorporating Fibers and Polymers. *J. Mater. Civ. Eng.* **2014**, *26*, 554–558. [CrossRef]
39. Ghuzlan, K.A.; Carpenter, S.H. Energy-Derived, Damage-Based Failure Criterion for Fatigue Testing. *Transp. Res. Rec.* **2000**, *1723*, 141–149. [CrossRef]
40. Dattoma, V.; Giancane, S. Evaluation of energy of fatigue damage into GFRC through digital image correlation and thermography. *Compos. Part B Eng.* **2013**, *47*, 283–289. [CrossRef]
41. Amin, A. Post Cracking Behaviour of Steel Fibre Reinforced Concrete: From Material to Structure. Ph.D. Thesis, the University of New South Wales, Sydney, Australia, 2015.

42. Foster, S.; Htut, T.; Ng, T. High performance fibre reinforced concrete: Fundamental behaviour and modelling. In Proceedings of the 8th International Conference on Fracture Mechanics of Concrete and Concrete Structures, FraMCoS 2013, Ciudad Real, Spain, 10–14 March 2013; pp. 69–78.
43. Htut, T. Fracture Processes in Steel Fibre Reinforced Concrete. Ph.D. Thesis, the University of New South Wales, Sydney, Australia, 2010.
44. Parvez, A. Fatigue Behaviour of Steel-Fibre-Reinforced Concrete Beams and Prestressed Sleepers. Ph.D. Thesis, the University of New South Wales, Sydney, Australia, 2015.

Publisher's Note: MDPI stays neutral with regard to jurisdictional claims in published maps and institutional affiliations.



© 2020 by the authors. Licensee MDPI, Basel, Switzerland. This article is an open access article distributed under the terms and conditions of the Creative Commons Attribution (CC BY) license (<http://creativecommons.org/licenses/by/4.0/>).